EXTENDED PDF FORMAT
SPONSORED BY
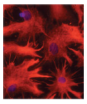
Travel Grants Available
Neuroscience 2014
Application Deadline: July 31st
>Apply Now
R&D systems
a bio-techne brand
www.rndsystems.com

Genomic basis for the convergent evolution of electric organs

Jason R. Gallant *et al.*

Science **344**, 1522 (2014);
DOI: 10.1126/science.1254432

This copy is for your personal, non-commercial use only.

If you wish to distribute this article to others, you can order high-quality copies for your colleagues, clients, or customers by clicking here.

Permission to republish or repurpose articles or portions of articles can be obtained by following the guidelines here.

The following resources related to this article are available online at www.sciencemag.org (this information is current as of July 3, 2014):

Updated information and services, including high-resolution figures, can be found in the online version of this article at:
http://www.sciencemag.org/content/344/6191/1522.full.html

Supporting Online Material can be found at:
http://www.sciencemag.org/content/suppl/2014/06/25/344.6191.1522.DC1.html

This article **cites 78 articles**, 35 of which can be accessed free:
http://www.sciencemag.org/content/344/6191/1522.full.html#ref-list-1

This article appears in the following **subject collections:**
Evolution
http://www.sciencemag.org/cgi/collection/evolution

Downloaded from www.sciencemag.org on July 3, 2014

Science (print ISSN 0036-8075; online ISSN 1095-9203) is published weekly, except the last week in December, by the American Association for the Advancement of Science, 1200 New York Avenue NW, Washington, DC 20005. Copyright 2014 by the American Association for the Advancement of Science; all rights reserved. The title *Science* is a registered trademark of AAAS.

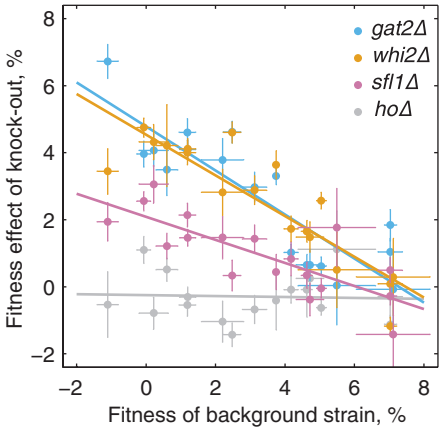

Fig. 3. Diminishing-returns epistasis among specific mutations. The fitness effect of knocking out genes *gat2*, *whi2*, and *sfl1* declines with the fitness of the background strain. The *ho* knockout is a negative control. Error bars are SEM over biological replicates.

leads to a striking pattern of convergent evolution, making fitness evolution relatively predictable. Despite this fitness-level convergence, evolution remains highly stochastic at the genotype level, likely because many distinct mutational paths can lead a population to any given fitness.

REFERENCES AND NOTES

1. R. J. Woods *et al.*, *Science* **331**, 1433–1436 (2011).
2. Z. D. Blount, C. Z. Borland, R. E. Lenski, *Proc. Natl. Acad. Sci. U.S.A.* **105**, 7899–7906 (2008).
3. J. D. Bloom, L. I. Gong, D. Baltimore, *Science* **328**, 1272–1275 (2010).
4. D. R. Rokyta *et al.*, *PLOS Genet.* **7**, e1002075 (2011).
5. C. L. Burch, L. Chao, *Nature* **406**, 625–628 (2000).
6. D. M. Weinreich, N. F. Delaney, M. A. Depristo, D. L. Hartl, *Science* **312**, 111–114 (2006).
7. S. J. Gould, *Wonderful Life* (Norton, New York, 1989).
8. A. I. Khan, D. M. Dinh, D. Schneider, R. E. Lenski, T. F. Cooper, *Science* **332**, 1193–1196 (2011).
9. H.-H. Chou, H.-C. Chiu, N. F. Delaney, D. Segrè, C. J. Marx, *Science* **332**, 1190–1192 (2011).
10. H.-H. Chou, J. Berthet, C. J. Marx, *PLOS Genet.* **5**, e1000652 (2009).
11. J. E. Barrick, M. R. Kauth, C. C. Strelioff, R. E. Lenski, *Mol. Biol. Evol.* **27**, 1338–1347 (2010).
12. L. Perfeito, A. Sousa, T. Bataillon, I. Gordo, *Evolution* **68**, 150–162 (2014).
13. M. J. Wiser, N. Ribeck, R. E. Lenski, *Science* **342**, 1364–1367 (2013).
14. O. Tenaillon *et al.*, *Science* **335**, 457–461 (2012).
15. G. I. Lang, D. Botstein, M. M. Desai, *Genetics* **188**, 647–661 (2011).
16. See supplementary materials on *Science* Online.
17. M. Travisano, J. A. Mongold, A. F. Bennett, R. E. Lenski, *Science* **267**, 87–90 (1995).
18. S. Kryazhimskiy, G. Tkačik, J. B. Plotkin, *Proc. Natl. Acad. Sci. U.S.A.* **106**, 18638–18643 (2009).
19. Note that this includes two founders inadvertently picked from the same diversified population (*16*).
20. J. P. Bollback, J. P. Huelsenbeck, *Mol. Biol. Evol.* **24**, 1397–1406 (2007).
21. G. I. Lang *et al.*, *Nature* **500**, 571–574 (2013).
22. This result is also surprising in the diminishing-returns models because we expect fewer beneficial mutations to fix in high-fitness backgrounds where they provide a smaller selective advantage. This puzzle is related to the observation (*25*) that fixation rates in long-term evolution of *E. coli* are constant through time despite a declining rate of fitness increase. However, our result would be consistent with the diminishing-returns models if the beneficial mutation rate is also higher in high-fitness backgrounds.
23. See (*16*) for a power analysis.
24. These are likely enriched for the most strongly beneficial mutations. Hence, if modular epistasis is prevalent, it is among these mutations that we expect the strongest trend.
25. J. E. Barrick *et al.*, *Nature* **461**, 1243–1247 (2009).

ACKNOWLEDGMENTS

We thank A. Murray, Q. Justman, B. Good, D. van Dyken, M. McDonald for useful discussions; A. Subramaniam, G. Lang, M. Müller, and J. Koschwanez for experimental advice and strains; and P. Rogers and C. Daly for technical support. Supported by the Burroughs Wellcome Foundation (S.K.), NSF graduate research fellowships (D.P.R., E.R.J.), and the James S. McDonnell Foundation, the Alfred P. Sloan Foundation, the Harvard Milton Fund, NSF grant PHY 1313638, and NIH grant GM104239 (M.M.D.). Sequence data have been deposited to GenBank under BioProject identifier PRJNA242140.

SUPPLEMENTARY MATERIALS

www.sciencemag.org/content/344/6191/1519/suppl/DC1
Materials and Methods
Figs. S1 to S12
Tables S1 to S12
References (*26*–*34*)

16 January 2014; accepted 28 May 2014
10.1126/science.1250939

NONHUMAN GENETICS

Genomic basis for the convergent evolution of electric organs

Jason R. Gallant,[1,2]* Lindsay L. Traeger,[3,4]* Jeremy D. Volkening,[4,5] Howell Moffett,[6,7] Po-Hao Chen,[6,7,8] Carl D. Novina,[6,7,8] George N. Phillips Jr.,[9] Rene Anand,[10] Gregg B. Wells,[11] Matthew Pinch,[12] Robert Güth,[12] Graciela A. Unguez,[12] James S. Albert,[13] Harold H. Zakon,[2,14,15]† Manoj P. Samanta,[16]† Michael R. Sussman[4,5]†

Little is known about the genetic basis of convergent traits that originate repeatedly over broad taxonomic scales. The myogenic electric organ has evolved six times in fishes to produce electric fields used in communication, navigation, predation, or defense. We have examined the genomic basis of the convergent anatomical and physiological origins of these organs by assembling the genome of the electric eel (*Electrophorus electricus*) and sequencing electric organ and skeletal muscle transcriptomes from three lineages that have independently evolved electric organs. Our results indicate that, despite millions of years of evolution and large differences in the morphology of electric organ cells, independent lineages have leveraged similar transcription factors and developmental and cellular pathways in the evolution of electric organs.

Electric fishes use electric organs (EOs) to produce electricity for the purposes of communication; navigation; and, in extreme cases, predation and defense (*1*). EOs are a distinct vertebrate trait that has evolved at least six times independently (Fig. 1A). The taxonomic diversity of fishes that generate electricity is so profound that Darwin specifically cited them as an important example of convergent evolution (*2*). EOs benefit as a model for understanding general principles of the evolution of complex traits, as fish have evolved other specialized noncontractile muscle-derived organs (*3*). Furthermore, EOs provide a basis to assess whether similar mechanisms underlie the evolution of other specialized noncontractile muscle derivatives, such as the cardiac conduction system (*4*).

Electric organs are composed of cells called electrocytes (Fig. 1B). All electrocytes have an innervated surface enriched in cation-specific ion channels and, on the opposite surface, an invaginated plasma membrane enriched in sodium pumps, and, in some species, ion channels as well. The functional asymmetry of these cells, and their "in-series" arrangement within each organ, allows for the summation of voltages, much like batteries stacked in series in a flashlight. Although EOs originate developmentally from myogenic precursors, they are notably larger than muscle fibers (*5*). Further, they either lack the contractile machinery clearly evident in electron

[1]Department of Zoology, Michigan State University, East Lansing, MI 48824, USA. [2]BEACON Center for the Study of Evolution in Action, Michigan State University, East Lansing, MI 48824, USA. [3]Department of Genetics, University of Wisconsin, Madison, WI 53706, USA. [4]Biotechnology Center, University of Wisconsin, Madison, WI 53706, USA. [5]Department of Biochemistry, University of Wisconsin, Madison, WI 53706, USA. [6]Department of Cancer Immunology and AIDS, Dana-Farber Cancer Institute, Boston, MA 02115, USA. [7]Department of Microbiology and Immunobiology, Harvard Medical School, Boston, MA 02115, USA. [8]Broad Institute of Harvard and MIT, Cambridge, MA 02141, USA. [9]Department of Biochemistry and Cell Biology and Department of Chemistry, Rice University, Houston, TX 77005, USA. [10]Department of Pharmacology and Department of Neuroscience, College of Medicine, The Ohio State University Wexner Medical Center, Columbus, OH 43210, USA. [11]Department of Molecular and Cellular Medicine, Texas A&M University, College Station, TX 77843, USA. [12]Department of Biology, New Mexico State University, Las Cruces, NM 88003, USA. [13]Department of Biology, University of Louisiana, Lafayette, LA 70503, USA. [14]University of Texas, Austin, TX 78712, USA. [15]The Josephine Bay Paul Center for Comparative Molecular Biology and Evolution, The Marine Biological Laboratory, Woods Hole, MA 02543, USA. [16]Systemix Institute, Redmond, WA 98053, USA.
*These authors contributed equally to this work. **†Corresponding author. E-mail: msussman@wisc.edu (M.R.S.); manoj.samanta@systemix.org (M.P.S.); h.zakon@austin.utexas.edu (H.H.Z.)**

micrographs of muscle cells (Fig. 1B) or, if sarcomeres are present, as in mormyroid fish, they are disarrayed and noncontractile (Fig. 1B). Finally, electrocyte morphology varies widely: they can be long and slender, box-like, or flattened and pancake-like (Fig. 1B). Despite these differences in morphology, the three lineages of electric fish studied here share patterns of gene expression in transcription factors and pathways contributing to increased cell size, increased excitability, and decreased contractility.

We used next-generation sequencing technologies to construct a draft assembly of the *Electrophorus electricus* genome. Like all Gymnotiformes, *E. electricus* has a weak EO but is most famous for its distinct strong voltage EO. To inform gene predictions in the genome assembly, we generated short-read mRNA sequences from the main, Sachs', and Hunter's EOs, as well as the kidney, brain, spinal cord, skeletal muscle, and heart (*6*). This resulted in 29,363 gene models representing an estimated 22,000 protein-coding genes (table S1). Variance filtering of the gene models removed genes with low covariance among tissues, and

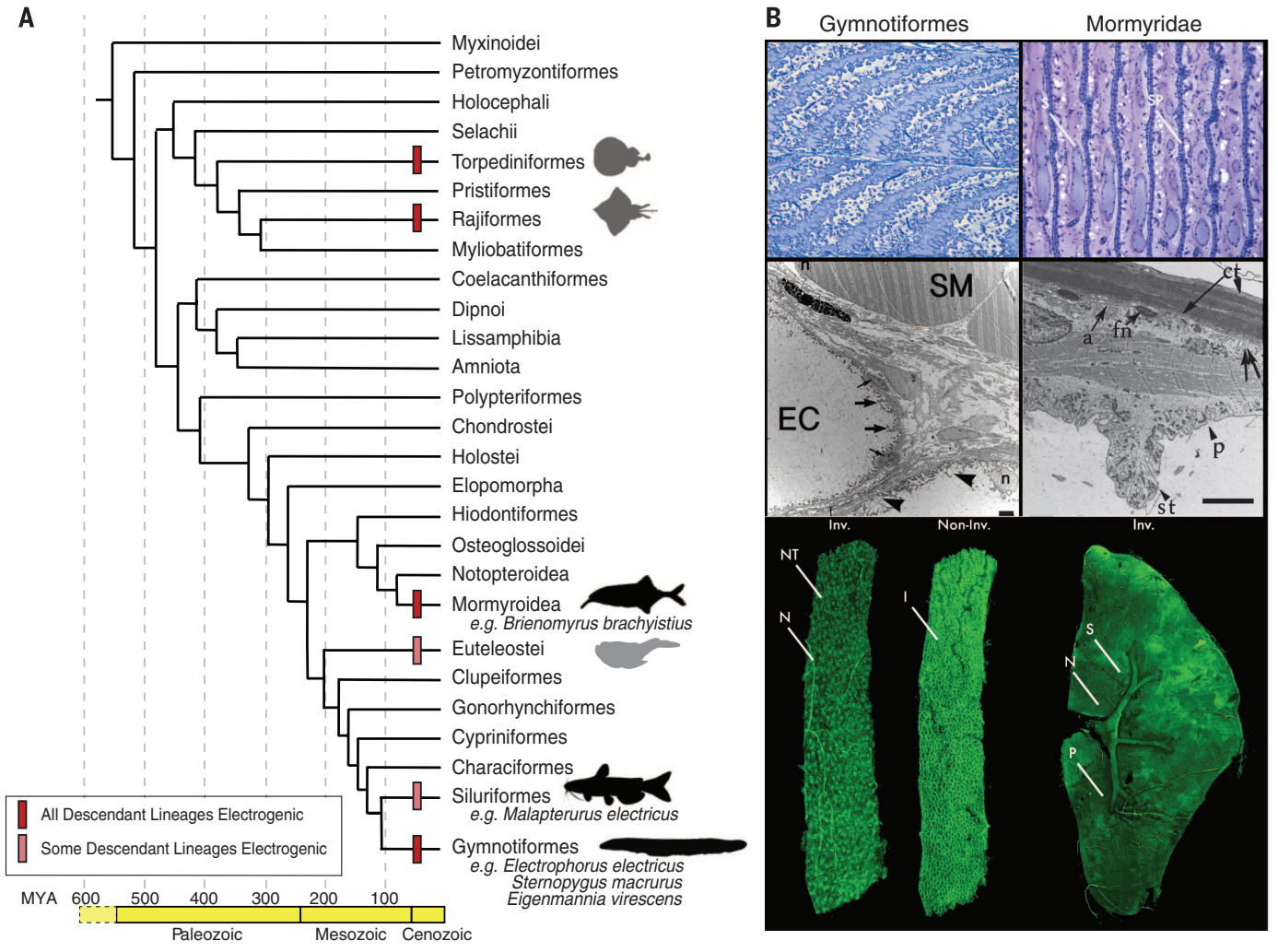

Fig. 1. Origins and diversity of EOs in vertebrates. (**A**) Phylogenetic tree of vertebrate orders and major groups of electric fishes, after (*25*). Geological periods and ages [in million years ago (MYA)] are shown at bottom. The origins of electrogenesis are indicated with bars (see legend) at internal branches. Black silhouettes denote lineages surveyed in the present study; gray silhouettes represent electrogenic lineages that were not surveyed. (**B**) (Top left) Sagittal sections through the *E. electricus* EO for the innervated, invaginated face and uninnervated smooth faces of the electrocyte and their in-series arrangement. (Top right) Sagittal section through the EO of the mormyroid *Paramormyrops kingsleyae*. Anterior is left; posterior is right. In mormyroids, innervation is restricted to a narrow region of the stalk system (S) protruding from the innervated, anterior face of the electrocyte. Also note the central filament of sarcomeric proteins (SP) between the multinucleated electrocyte faces. (Middle left) An electron micrograph of both skeletal muscle (SM) and electrocytes (EC) from the gymnotiform *S. macrurus*, which contain an amorphous cytoplasm devoid of sarcomeres: the striated, contractile structures that fill the cytosol of muscle cells. Peripheral nuclei (n) are marked in both electrocyte and muscle cells. In electrocytes, thick arrows point to mitochondria, thin arrows point to satellite cells, and arrowheads mark membrane-bound vesicular structures. Scale bar, 2 μm. (Middle right) An electron micrograph of an electrocyte of the mormyroid *P. kingsleyae*, illustrating the disorganized sarcomeric proteins in the center of the electrocyte. The outer edge of an electrocyte forms a "footplate" that apposes the connective tissue sheath (ct) surrounding the EO. The anterior face (a) of the electrocyte forms the major surface of the plate lying against the connective tissue surface. Fibroblast nuclei (fn), papillae (p), and stalk (st) are also indicated. Double arrows correspond to invaginations of the posterior face. Scale bar, 4 μm. [Image provided by Andrew Bass (Cornell University)] (Bottom left) A confocal reconstruction of an *E. electricus* electrocyte from anterior and posterior views. The nerve (N) innervating the innervated (Inv.) face is clearly visible, along with the many cholinergic nerve terminals (NT). The numerous invaginations (I) of the noninnervated (Non-Inv.) face are visible. (Bottom right) A confocal reconstruction of a *P. kingsleyae* electrocyte, clearly showing the protruding stalk system (S) from the anterior face. The stalk junction is innervated by motoneurons (N) in a highly localized fashion to contrast with *E. electricus*. Penetrations (P) are also visible in the electrocyte face.

subsequent *k*-means clustering (k = 12) revealed sets of tissue-specific cotranscriptionally regulated genes (*6*) (fig. S1). We focused primarily on a reduced set of genes that were highly up-regulated only in EOs (cluster 9, 211 genes) or down-regulated in EOs compared with skeletal and heart muscle (cluster 1, 186 genes).

Next, we sequenced and performed de novo assembly of the transcriptomes from EOs and skeletal muscles in two other Gymnotiformes from South America (*Sternopygus macrurus* and *Eigenmannia virescens*), as well as in two other species with independently evolved EOs, a mormyroid from Africa (*Brienomyrus brachyistius*) and the electric catfish from Africa (*Malapterurus electricus*). For each species, we assigned orthology between transcripts by reciprocal BLAST searching of the set of *E. electricus* genes followed by manual confirmation of the matches (*6*). We focused on convergent properties of EOs versus skeletal muscle among lineages, and we then examined patterns of gene expression in transcription factors and developmental pathways to determine candidate mechanisms underlying these similarities (Fig. 2). We highlighted genes likely to be involved in phenotypic characteristics of electrocytes relative to muscle, including (i) down-regulation of myogenic transcriptional "profile," (ii) increased excitability, (iii) enhanced insulation, (iv) elimination of excitation-contraction coupling, and (v) large size.

We found elevated expression of several transcription factors (Fig. 2 and fig. S2) expressed early in muscle differentiation (*7*) that are typically down-regulated in skeletal muscle after differentiation. *Six2a* is of particular interest, given that it is known to target ARE promoter elements in Na^+/K^+ adenosine triphosphatases (*8*, *9*). Concordant with the expression of early muscle transcription factors is the down-regulation of some transcription factors involved in muscle differentiation (e.g., *myogenin* and *six4b*) in *E. electricus*, *B. brachyistius*, and *M. electricus*, although not in the gymnotiform *S. macrurus*. Interestingly, *hey1*, which is one of the most consistent highly up-regulated genes in the EOs across all groups of electric fishes, is abundant in zebrafish somites and down-regulated in mature muscle, and its overexpression in mammalian muscle precursor cells prevents their

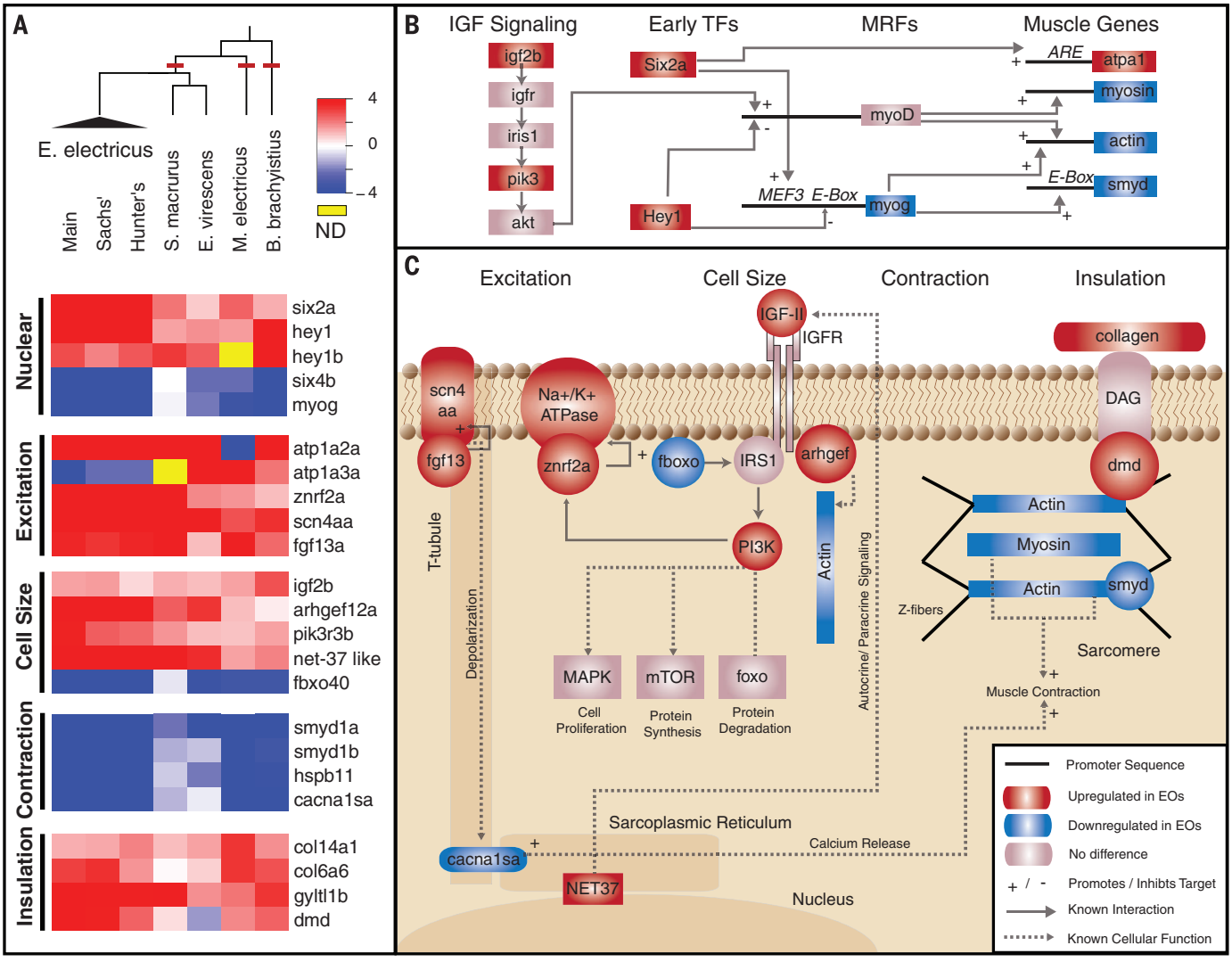

Fig. 2. Common toolkit for convergent evolution of EOs. (**A**) RNA-Seq was performed on five species, representing three independent origins of electrogenesis (cladogram, red lines). Also shown are plots of the log-transformed ratio of EO to skeletal muscle expression genes (red, up-regulated in EO; blue, down-regulated in EO) in several categories of function, including (i) nuclear transcription factors, (ii) genes that regulate cell excitation, (iii) genes that regulate cell size, (iv) genes involved in contraction and excitation contraction coupling, and (v) genes encoding proteins that surround individual electrocytes to provide the scaffold for insulation. *hey1b* data for *E. electricus* was derived from the Trinity transcriptome assembly (*6*). (**B**) Interaction of identified IGF signaling and transcription factors (TFs). IGF signaling pathway genes and early TFs influence the expression of muscle regulatory factors (MRFs), which ultimately lead to the expression of muscle-specific effector genes (table S3). (**C**) Interactions of genes identified in (A) are shown, grouped by function. For each, we list known patterns of expression in electric fish or the result of knockout studies in other vertebrates (table S4). IGFR, IGF receptor; MAPK, mitogen-activated protein kinase.

differentiation into muscle (*10*). Furthermore, *hey1* is transiently expressed in the developing cardiac conduction pathway, and its overexpression in the heart prevents assembly of the sarcomeres (*4*).

A key feature of EOs is that current dissipation must be minimized and conducted unidirectionally from the EOs through the body of the fish and into the water. We noted two collagen genes, *col6a6* and *col14a1*, that are up-regulated in EOs. The first is associated with muscle fibers, and the second is more generally expressed and ties the collagen fibers together. Collagen is deposited in the extracellular domain of basal lamina and is maintained by a cluster of molecules that span the membrane and attach to the cytoskeleton. Two of these membrane-spanning proteins, including a glycosyltransferase (*gyltl1b*) and dystrophin (mutations of which cause muscular dystrophy) (*11*), are also up-regulated in EOs and are probably involved in assembling the components that direct the flow of current.

Also, as expected, several transporters (*atp1a2a* or *atp1a3a*) and voltage-dependent ion channels (*scn4aa*) were highly expressed in all EOs, along with molecules that regulate them (*znrf2a* and *fgf13a*, respectively). Interestingly, the highly expressed gene encoding the α subunit of the sodium pump (*atp1a2a*) most closely resembles the isoform also expressed in transverse tubules (T-tubules) of muscle (*12*) and is abundant in the villi located within the invaginated side of the *E. electricus* electrocyte (*13*), suggesting that the uninnervated face of the electrocyte is derived from the T-tubule membrane.

A key step in the evolution of electrocytes requires disabling the excitation-contraction pathway. We noted variation in the extent to which genes for sarcomeric and sarcoplasmic reticulum–associated proteins are down-regulated in different species (Fig. 2, fig. S3, and table S2). Furthermore, mormyroid electrocytes still have sarcomere-like structures, although they appear disrupted (Fig. 1B). Despite these differences, the gene encoding the L-type calcium channel, or dihydropyridine receptor (*cacna1s*), which is localized in T-tubules and associated with excitation-contraction coupling in muscle, is down-regulated in all lineages. The *smyds* and *hspb11* genes are also down-regulated in all lineages. These proteins associate with the sarcomeres, and zebrafish and mice with reduced expression or mutant gene copies have disrupted sarcomeres (*14*). The observed low levels of these genes in EOs suggest that they may promote disassembly of the sarcomeres, and we hypothesize that the early evolution of the EO included the down-regulation of this suite of genes, disabling contraction.

As electrocytes are much larger than muscle fibers, we hypothesized that this might be due to changes in insulin-like growth factor (IGF) signaling pathway genes (Fig. 2 and fig. S4). IGF signaling enhances body size and developmental rate in an organism-wide and tissue-specific fashion (*15*–*18*). IGF ligands are produced and released by muscle in an autocrine fashion (*19*), and differences in IGF signaling may result in differential growth of muscles. IGF signaling activates the insulin receptor substrate 1 protein (IRS1), which then binds to the regulatory subunit of phosphoinositide 3 kinase (PIK3) (*20*). PIK3 acts through distinct signaling targets to regulate cell size, cell proliferation, and protein synthesis and degradation (*21*). The IGF pathway is also autoregulated by a muscle-specific protein, Fbxo40, which brings IRS1 to an E3 ligase complex. Thus, up-regulation of IRS1 is likely a key step in increasing IGF signaling activity in electrocytes.

Finally, the nuclear-envelope–related protein (Net37), abundant in cardiac and skeletal muscle tissues (*22*), regulates autocrine and/or paracrine release of IGF signaling and is required for myogenic differentiation of mouse myoblast cells (*23*). We detected electrocyte-specific up-regulation of *igf1l*, a gene for PI3K (*pik3r3b*) and a *net37*-like gene in all lineages, as well as down-regulation of the negative inhibitor *fbxo40*. The *net37*-like protein was also recently reported to be highly expressed in the EO of another electric fish, the *Torpedo* ray (*24*). Together, the observed changes in expression in these key IGF signaling pathway genes suggest a conserved pathway among electrocytes that contributes to their increased size. The independent changes and the resulting enhancement in cell size highlight these genes as possible intracellular effectors in other insulin- or IGF-sensitive systems, as observed in male horned beetles (*18*).

Our analysis suggests that a common regulatory network of transcription factors and developmental pathways may have been repeatedly targeted by selection in the evolution of EOs, despite their very different morphologies. Moreover, our work illuminates convergent evolution of EOs and emphasizes key signaling steps that may be foci for the evolution of tissues and organs in other organisms.

REFERENCES AND NOTES

1. J. S. Albert, W. G. R. Crampton, in *The Physiology of Fishes* (Springer, New York, ed. 3, 2005), pp. 431–472.
2. C. Darwin, in *On the Origin of Species by Means of Natural Selection* (J. Murray, London, 1859), pp. ix, 1.
3. B. A. Block, *Am. Zool.* **31**, 726–742 (1991).
4. H. Kokubo, S. Tomita-Miyagawa, Y. Hamada, Y. Saga, *Development* **134**, 747–755 (2007).
5. G. A. Unguez, H. H. Zakon, *J. Neurosci.* **18**, 9924–9935 (1998).
6. Materials and methods are available as supplementary materials on *Science* Online.
7. H. Ghanbari, H. C. Seo, A. Fjose, A. W. Brändli, *Mech. Dev.* **101**, 271–277 (2001).
8. F. Spitz *et al*., *Proc. Natl. Acad. Sci. U.S.A.* **95**, 14220–14225 (1998).
9. K. Kawakami *et al*., *Nature* **316**, 733–736 (1985).
10. M. F. Buas, S. Kabak, T. Kadesch, *J. Biol. Chem.* **285**, 1249–1258 (2010).
11. K. J. Nowak, K. E. Davies, *EMBO Rep.* **5**, 872–876 (2004).
12. R. G. Berry, S. Despa, W. Fuller, D. M. Bers, M. J. Shattock, *Cardiovasc. Res.* **73**, 92–100 (2007).
13. J. Lowe *et al*., *Biochim. Biophys. Acta* **1661**, 40–46 (2004).
14. N. Klüver *et al*., *PLOS ONE* **6**, e29063 (2011).
15. C. Duan, H. Ren, S. Gao, *Gen. Comp. Endocrinol.* **167**, 344–351 (2010).
16. B. C. Hoopes, M. Rimbault, D. Liebers, E. A. Ostrander, N. B. Sutter, *Mamm. Genome* **23**, 780–790 (2012).
17. N. B. Sutter *et al*., *Science* **316**, 112–115 (2007).
18. D. J. Emlen, I. A. Warren, A. Johns, I. Dworkin, L. C. Lavine, *Science* **337**, 860–864 (2012).
19. A. S. Van Laere *et al*., *Nature* **425**, 832–836 (2003).
20. I. Mothe *et al*., *Mol. Endocrinol.* **11**, 1911–1923 (1997).
21. A. Otto, K. Patel, *Exp. Cell Res.* **316**, 3059–3066 (2010).
22. I. H. Chen, M. Huber, T. Guan, A. Bubeck, L. Gerace, *BMC Cell Biol.* **7**, 38 (2006).
23. K. Datta, T. Guan, L. Gerace, *J. Biol. Chem.* **284**, 29666–29676 (2009).
24. S. E. Mate, K. J. Brown, E. P. Hoffman, *Skeletal Muscle* **1**, 20 (2011).
25. M. E. Alfaro *et al*., *Proc. Natl. Acad. Sci. U.S.A.* **106**, 13410–13414 (2009).

ACKNOWLEDGMENTS

This project has been funded in part by NSF grants MCB no. 1144012 (M.R.S.), CNS no. 1248109 (G.A.U.), and DEB no. 0741450 (J.S.A.); the W.M. Keck Foundation Distinguished Young Scholars in Medical Research (C.D.N.); NIH grants R01 GM084879 (H.H.Z.), R01 GM088670 (R.A.), and 1SC1GM092297-01A1 (G.A.U.); the Texas A&M University Health Science Center College of Medicine (G.B.W.); the Cornell University Center for Vertebrate Genomics (J.R.G.); the University of Wisconsin Genetics NIH Graduate Training Grant (L.L.T.); and the Morgridge Graduate Fellowship (J.D.V.). E. V. Armbrust provided computing assistance, and S. B. McKay assisted with data analysis. M.P.S. acknowledges useful discussions with R. Chikhi, R. Luo, and J. Simpson. We thank J. Bayliss for dissection of *E. electricus* and R. Amasino for help in preparing this manuscript. M.R.S. and L.L.T. acknowledge the guidance of J. Hyman, M. Adams, and J. Speers from the University of Wisconsin Biotechnology Center for their excellent assistance in *E. electricus* sequencing. The raw sequencing reads have been deposited in the National Center for Biotechnology Information short-read archive for the *E. electricus* genome (BioProject ID: PRJNA249073) and transcriptome sequences of *E. electricus*, *S. macrurus*, *E. virescens*, *M. electricus*, and *B. brachyistius* (BioProject ID: PRJNA248545). The whole-genome assemblies and annotation, together with the transcriptome assemblies, are available at http://efishgenomics.zoology.msu.edu, along with BLAST and genome-browsing services.

SUPPLEMENTARY MATERIALS

www.sciencemag.org/content/344/6191/1522/suppl/DC1
Materials and Methods
Supplementary Text
Figs. S1 to S6
Tables S1 to S7
References (*26*–*91*)

7 April 2014; accepted 6 June 2014
10.1126/science.1254432